



1 **Novel two-component regulatory systems play a role in biofilm formation of**  
2 ***Lactobacillus reuteri* rodent isolate 100-23**

3 Marcia Shu-Wei Su<sup>1,2</sup> and Michael G. Gänzle<sup>1\*</sup>.

4 **Running title: Two component systems and biofilms in *L. reuteri***

5 **Contents category: Cell and Molecular Biology of Microbes**

6

7 <sup>1</sup> University of Alberta, Dept. of Agricultural, Food and Nutritional Science,  
8 Edmonton, AB, Canada.

9 <sup>2</sup> Present address: Pennsylvania State University, Department of Biology,  
10 University Park, PA 16802, USA

11 # of words in abstract: 199.

12 # of words in text: 5117

13 # of tables and figures: 2 tables, 5 figures

14 Accession numbers of any gene sequences are included at the end of the materials  
15 and methods section.

16 \* corresponding author footnote:

17 Michael Gänzle, University of Alberta, Dept. of Agricultural, Food, and

18 Nutritional Science, 4-10 Ag/For Centre, Edmonton, AB, T6G 2P5, Canada.

19 Phone: + 1 780 492 0774; fax: + 1 780 492 4265; e-mail: [mgaenzle@ualberta.ca](mailto:mgaenzle@ualberta.ca)

20

21 **Abstract**

22           This study characterized the two-component regulatory systems encoded  
23 by *bfrKRT* and *cemAKR*, and assessed their influence on biofilm formation by *L.*  
24 *reuteri* 100-23. A method for deletion of multiple genes was employed to disrupt  
25 genetic loci of two component systems. The operons *bfrKRT* and *cemAKR* show  
26 complementary organization. Genes *bfrKRT* code for a histidine kinase, a  
27 response regulator, and an ATP-binding cassette-type transporter with a  
28 bacteriocin processing peptidase domain, respectively. Genes *cemAKR* code for a  
29 signal peptide, a histidine kinase, and a response regulator, respectively. Deletion  
30 of single or multiple genes in the operons *bfrKRT* and *cemAKR* did not affect cell  
31 morphology, growth, or the sensitivity to various stressors. However, gene  
32 disruption affected biofilm formation, this effect was dependent on the carbon  
33 source. Deletion of *bfrK* or *cemA* increased sucrose-dependent biofilm formation  
34 *in vitro*. Glucose-dependent biofilm formation was particularly increased by  
35 deletion of *cemK*. The expression of *cemK* and *cemR* was altered by deletion of  
36 *bfrK*, indicating cross-talk between these two regulatory systems. These results  
37 may contribute to our understanding of the genetic factors related to the biofilm  
38 formation and competitiveness of *L. reuteri* in intestinal ecosystems.

39 **Key words:** *Lactobacillus reuteri*, two-component regulatory systems, biofilm  
40 formation, multi-deletion mutagenesis

41

42 **Introduction**

43 *Lactobacillus reuteri* a lactic acid bacterium that has adapted to the  
44 gastrointestinal tracts of vertebrates but also occurs in cereal fermentations (Vogel  
45 *et al.*, 1999; Walter *et al.*, 2011). The competitiveness of *L. reuteri* in cereal  
46 fermentations is based on carbohydrate and amino acid metabolism matching the  
47 substrate supply in cereals (Schwab *et al.*, 2007; Su *et al.*, 2011; Vogel *et al.*,  
48 1999). Sourdough isolates of *L. reuteri* share phylogenetic and physiological  
49 characteristics with intestinal strains of *L. reuteri* (Su *et al.*, 2012). *L. reuteri*  
50 colonizes the human gastrointestinal tract and the human female urogenital tract,  
51 and the upper intestinal tract of animals, including pigs, birds, and rodents (Fuller,  
52 1973; Fuller & Brooker, 1974; Fuller *et al.*, 1978; Savage *et al.*, 1968; Wesney &  
53 Tannock, 1979; for review, see Walter, 2008). Because of its stable association  
54 with vertebrate hosts, *L. reuteri* has been used as a model organism to study host-  
55 microbe interaction and host-specific adaptation (Frese *et al.*, 2011; Walter *et al.*,  
56 2011).

57 The colonization of animals by *L. reuteri* involved the formation of  
58 biofilms on non-secretory stratified squamous epithelia in the upper intestinal  
59 tract, e.g. the forestomach of mice and horses, and the crops of birds (Fuller &  
60 Brooker, 1974; Yuki *et al.*, 2000; Walter *et al.*, 2011). Biofilm formation is  
61 comprised of four major steps: adherence of cells to surfaces, cell accumulation,  
62 clonal maturation, and formation of mixed species biofilms (for reviews, see  
63 Karatan & Watnick, 2009; Nobbs *et al.*, 2009). In the first steps, adhesins  
64 facilitate adherence to surfaces. In the latter steps, quorum sensing,

65 exopolysaccharide formation, coaggregation, and genetic exchange play  
66 important roles. Adhesion of *L. reuteri* to the murine intestinal tract was mediated  
67 by a large surface protein (Frese *et al.*, 2011; Walter *et al.*, 2005). The mucus  
68 adhesion-promoting protein (referred to as MapA, CnBP, CyuC, or BspA)  
69 (Miyoshi *et al.*, 2006), and the mucus-binding protein (Mub) (Roos & Jonsson,  
70 2002) mediated adherence of *L. reuteri* to porcine intestinal mucus or human  
71 epithelial cells. Extracellular polysaccharides produced by the reuteransucrase of  
72 *L. reuteri* promoted biofilm formation in the murine forestomach and  
73 fructansucrases of *L. reuteri* acted as matrix-binding proteins (Sims *et al.*, 2011;  
74 Walter *et al.*, 2008). Biofilm formation by *L. reuteri* thus shares similarity with  
75 the oral pathogen *Streptococcus mutans*, which is ecotypically and  
76 phylogenetically related to *L. reuteri* (Zhang *et al.*, 2011). In *S. mutans*, biofilm  
77 formation is mediated by glucansucrases and fructansucrases and their expression  
78 is dependent on signal transduction by two-component systems (Nobbs *et al.*,  
79 2009; Quivey *et al.*, 2001; Senadheera *et al.*, 2007).

80         A typical two-component system consists of a histidine kinase that  
81 autophosphorylates in response to environmental stimuli and relays a phosphoryl  
82 group to its cognate response regulator. The response regulator then binds to  
83 DNA and alters gene expression (Mitrophanov & Groisman, 2008). A histidine  
84 kinase coded by gene *lr70430*, is unique to the rodent isolates of *L. reuteri* and  
85 contributes to the colonization of the rodent strain *L. reuteri* 100-23 in the murine  
86 forestomach (Frese *et al.*, 2011; Wesney & Tannock, 1979). However, the role of  
87 two component systems in the adaptation of *L. reuteri* to different hosts remains

88 to be elucidated. It was therefore the aim of this study to characterize the role of  
89 two-component systems in *L. reuteri* rodent isolate 100-23. A novel method for  
90 the multi-deletion mutagenesis in *L. reuteri* was employed. The genetic loci of  
91 two component systems were disrupted by homologous recombination. The  
92 phenotypes of deleted mutant strains, including their ability to adhere in the  
93 presence of glucose or sucrose, were characterized, and the regulatory signaling  
94 cascade was elucidated. Biofilm formation by *L. reuteri* 100-23 was compared to  
95 *L. reuteri* TMW1.106, a strain for which sucrose-dependent biofilm was  
96 described (Walter *et al.*, 2008).

## 97 **Materials and methods**

### 98 **Bacterial growth**

99 Bacterial strains and plasmids used in this study are listed in Table 1 and Table  
100 S1. *Escherichia coli* JM109 (Promega, Nepean, Canada) was cultured at 37°C in  
101 Luria-Bertani (LB) broth with agitation. *E. coli* harbouring pJRS233-derived  
102 plasmids was cultured in LB containing ampicillin (100 mg l<sup>-1</sup>) and erythromycin  
103 (500 mg l<sup>-1</sup>) at 30°C to maintain the plasmids. *L. reuteri* was cultured at 37°C  
104 under micro-aerobic conditions (1% O<sub>2</sub>, 5% CO<sub>2</sub>, and 94% N<sub>2</sub>) in deMan-Rogosa-  
105 Sharpe broth (MRS) (Difco, Becton Dickinson, Mississauga, Canada) unless  
106 otherwise specified. MRS media were modified as follows for specific  
107 experiments: mMRS (Gänzle *et al.*, 2000) containing 2% glucose as sole carbon  
108 source (gluMRS), and mMRS containing 2% sucrose as sole carbon source  
109 (sucMRS). Erythromycin (10 mg l<sup>-1</sup>) was added to MRS to grow erythromycin-  
110 resistant *L. reuteri*.

111 **DNA isolation and manipulation**

112 Genomic DNA was isolated using the Blood & Tissue Kit (Qiagen, Mississauga,  
113 Canada) according to the protocol provided by the manufacturer.  
114 Oligonucleotides (Table S2) were purchased from Integrated DNA Technologies  
115 (San Diego, CA). Restriction enzymes (New England Biolabs, Pickering,  
116 Canada), T4 DNA ligase (Epicentre, Markham, Canada), and Taq DNA  
117 polymerase (Invitrogen, Burlington, Canada) were used for cloning. DNA  
118 sequencing was performed after polymerase chain reaction (PCR) cloning (TA  
119 Vector, Invitrogen) (Macrogen, Rockville, MD).

120 **Bioinformatic analyses**

121 A web-based bacteriocin genome mining tool (BAGEL) (de Jong *et al.*, 2006)  
122 was used to predict sensing peptide-based two-component systems in lactobacilli.  
123 The similarity of nucleotide sequences was determined by pairwise sequence  
124 alignment using EMBOSS Water- Alignment. BLASTP analysis was performed  
125 to retrieve homologous proteins, which were further analyzed with Kyoto  
126 Encyclopedia of Genes and Genomes (KEGG) databases. Amino acid sequences  
127 were retrieved from UniProt (Bairoch *et al.*, 2005) and aligned to calculate their  
128 identity scores using MUSCLE pairwise alignment (Geneious version 5.6.6;  
129 Auckland, New Zealand). Protein function was predicted with the DAS program  
130 to define the transmembrane segments, the InterProscan program, Pfam, and the  
131 SMART method to find motifs and protein domains.

132 **Generation of *L. reuteri* knockout mutants**

133 The in-frame deletion method for generating *L. reuteri* knockout mutants has been  
134 described in a previous study (Su *et al.*, 2011). Plasmids and primers used are  
135 listed in Table S2 and Table S3, respectively, of the online supplementary  
136 material. In brief, the 5'- and 3'-flanking sequences of the target genes were  
137 amplified by PCR, and were thereafter referred to as amplicon-A and amplicon-B,  
138 respectively. Amplicon-A and amplicon-B were inserted separately into  
139 pGEMTeasy vectors to produce pGene-A and pGene-B. Next, the restriction  
140 enzymes (RE) were used to cut out two amplicons from pGene-A and pGene-B.  
141 These two amplicons were then ligated into a pGEMTeasy vector using T4 DNA  
142 ligase, which produced pGene-AB. The ligated DNA fragment AB was cut out of  
143 pGene-AB with suitable RE, and inserted into the integration shuttle vector  
144 pJRS233 (Perez-Casal *et al.*, 1993) to generate a knockout plasmid, pKO-*Gene-*  
145 *AB*. After electro-transforming pKO-*Gene-AB* into the *L. reuteri* wild type strain,  
146 a single-gene knockout mutant was generated by temperature-impulse integration  
147 and a plasmid-curing test as described by Su *et al.* (2011). An antibiotic-sensitive  
148 knockout mutant was identified by replica-plating onto mMRS and mMRS-  
149 erythromycin agar plates. The truncation of the target gene in the derived deletion  
150 mutant was confirmed by PCR with primer set *gene-KO-1* and *gene-KO-4*, and  
151 primer set *gene-5-F* and *gene-6-R*. The deletion of this region was confirmed by  
152 Sanger sequencing using primers *gene-5-F* and *gene-6-R*. The same strategy was  
153 used to generate double-gene knockout mutants and detailed in the supplementary  
154 material.

#### 155 **Scanning electron microscope (SEM) analysis of biofilm specimens**



156 *L. reuteri* 100-23, 100-23 $\Delta$ *cemK* $\Delta$ *cemR*, TMW1.106, and TMW1.106 $\Delta$ *gtfA* were  
157 grown on polystyrene plates containing gluMRS or sucMRS broth. After  
158 incubation, cells were washed with buffer containing 50 mM NaH<sub>2</sub>PO<sub>4</sub> (pH 6),  
159 and fixed with 2.5% glutaraldehyde in 10 mM of PBS buffer (pH 7.4) at 4°C  
160 overnight. Fixed cells were washed twice in PBS buffer and dehydrated by adding  
161 a series of one mL volumes of an increasingly concentrated ethanol in water  
162 solution (70, 85, 95, 100, and 100%, v/v) at room temperature. Cells were  
163 incubated in each ethanol concentration for 10 minutes. Hexamethyldisilazane  
164 (HMDS) (Sigma-Aldrich, Munich, Germany) was introduced into the cells by  
165 gradually increasing the concentration of HMDS in ethanol. The following series  
166 of HMDS in ethanol solutions was used: 75% ethanol/25% HMDS, 50%  
167 ethanol/50% HMDS, 25% ethanol/75% HMDS, and three volumes of 100%  
168 HMDS. Samples were air-dried overnight and then broken down into smaller  
169 pieces that were later mounted on SEM stubs, where they were immediately  
170 coated with Au/Pd on a sputter coater (Hummer 6.2) (Anatech, Union City,  
171 California). The examination was performed using a scanning electron  
172 microscope XL30 (FEI, Hillsboro, Oregon) at an acceleration voltage of 20 kV.

### 173 **RNA extraction**

174 The MasterPure™ RNA Purification protocol (Epicentre Technologies,  
175 Markham, Canada) was used with slight modifications. Overnight cultures of *L.*  
176 *reuteri* were diluted fifty-fold in gluMRS broth and incubated at 37°C until an  
177 OD<sub>600nm</sub> of 0.4 was reached. Cells from 10 ml of culture were harvested and RNA  
178 synthesis was halted by adding 1.25 ml of ice-cold ethanol/phenol Stop Solution

179 (5% acidic phenol in ethanol, pH < 7). Cells were harvested by centrifugation and  
180 lysed at 65°C for 15 min with 300 µl of Tissue and Cell Lysis Solution containing  
181 5.5 µg of Proteinase K. After incubation on ice for five min, 175 µl of MPC  
182 Protein Precipitation Reagent was added to denature proteins, followed by  
183 centrifugation at 10 000 × g for 10 minutes. The supernatant was mixed with 500  
184 µl of isopropanol and nucleic acids were collected by centrifugation. The resulting  
185 pellets were rinsed with a 75% ethanol solution, suspended in 30 µl of nuclease-  
186 free water (Ambion), and treated with RNase-free DNase I (Ambion, Streetsville,  
187 Canada) at 37°C for 2 h. The reaction was stopped by addition of 5 µl of 50 mM  
188 EDTA. Five units of SUPERase·In (RNase inhibitor, Ambion) were added and  
189 the RNA was stored at 4°C.

#### 190 **Complementary DNA synthesis**

191 Two µg of RNA was used as a template for cDNA synthesis using Random  
192 Primers (Invitrogen), dNTPs (Invitrogen), and nuclease-free water (Ambion). The  
193 RNA/Primer mixture was incubated at 70°C for 10 minutes, then 25°C for 10  
194 minutes, and finally chilled to 4°C. The reaction mix was prepared with the  
195 RNA/Primer mixture, 5× 1<sup>st</sup> Strand Buffer, 100 mM DTT, SUPERase·In,  
196 SuperScript III (reverse transcriptase, Invitrogen), and nuclease-free water. This  
197 reaction mixture was then incubated at 25°C for 10 minutes, 37°C for 1 h, 42°C  
198 for 1 h, and then 70°C for 10 minutes to inactivate SuperScript III. The cDNAs  
199 were stored at 4°C. Amplifications were carried out in a GeneAmp PCR System  
200 9700 (Applied Biosystems, Streetsville, Canada).

#### 201 **Relative quantification of gene expression using quantitative PCR (qPCR)**

202 Gene expression was quantified with qPCR with cDNA as template. Gene-  
203 specific primers were designed to have amplicons of 90-150 bp in size using  
204 Primer Express Software 3.0 (Applied Biosystems). PCR was carried out with  
205 custom SYBR Green Master Mix (the MBSU facility, University of Alberta) in a  
206 7500 Fast Real-time PCR instrument (Applied Biosystems). The calculation of  
207 the relative gene expression was carried out according to the  $\Delta\Delta C_t$  method  
208 (Pfaffl, 2001). Exponentially growing cells of *L. reuteri* 100-23 were used as a  
209 reference condition, and *recA* was used as endogenous gene control. The PCR-  
210 efficiencies of the primers were experimentally determined with serial dilutions of  
211 the cDNA of *L. reuteri* 100-23 and calculated as described (Pfaffl, 2001) with  
212 ABI software. The amplification program was 95°C for 2 minutes, 40 cycles of  
213 95°C for 15 seconds, and 60°C for 1 minute. Data was collected at 60°C followed  
214 by a dissociation curve. Analysis was performed in triplicate technical repeats and  
215 three independent experiments. DNase I-treated RNA and genomic DNA were  
216 used as negative and positive controls, respectively.

### 217 **Adherence assay**

218 The adherence assay was based on the method of Loo *et al.* (Loo *et al.*, 2000)  
219 with modifications. Cells from cultures grown overnight were washed, sub-  
220 cultured in two milliliters of gluMRS or sucMRS media, and incubated in 35 mm  
221 x 10 mm polystyrene petri dishes. After 24 h of inoculation, the supernatants were  
222 discarded, and wells were washed twice with 50 mM NaH<sub>2</sub>PO<sub>4</sub> (pH 6) buffer.  
223 Cells adhering to the plate were scraped using plastic tips and resuspended in one  
224 milliliter of phosphate buffer. The cell density was determined by measuring the

225 OD<sub>600nm</sub>. Analysis was performed in triplicate independent experiments with two  
226 or three technical repeats per replicate.

### 227 **Statistical analysis**

228 Statistical analysis was performed using Student's *t*-test (SigmaPlot, version 11.0;  
229 Chicago, IL).

### 230 **Sequences and accession numbers**

231 The nucleotide sequence of the *bfrKRT* and *cemAKR* operons were retrieved from  
232 the GenBank database (accession number: NZ\_AAPZ00000000.2 ; locus tag:  
233 Lreu23DRAFT\_4807 for *bfrK*; Lreu23DRAFT\_4808 for *bfrR*;  
234 Lreu23DRAFT\_4809 for *bfrT*; Lreu23DRAFT\_4825 for *cemK*; and  
235 Lreu23DRAFT\_4826 for *cemR*). The nucleotide sequence of *cemA* is 5'-  
236 ATGCAAAAACATCAATTCATCAACTATCTTTAATTAAGGGTGGTATA  
237 TACTCACTTTTAAGTCTGTAAA-3', and the predicted protein sequence is  
238 MQKLSIHQLSLIKGGIYSLLSL. The nucleotide sequences of *L. reuteri* mutant  
239 strains were deposited to Genebank with the following accession numbers:  
240  $\Delta$ *cemA*, JF339968;  $\Delta$ *bfrK*, KF306072;  $\Delta$ *bfrK* $\Delta$ *bfrR*, KF306073;  $\Delta$ *cemK*,  
241 KF306074;  $\Delta$ *bfrR* KF306075;  $\Delta$ *cemK* $\Delta$ *cemR*, KF306076;  $\Delta$ *bfrR* $\Delta$ *cemK*,  
242 KF306077;  $\Delta$ *bfrK* $\Delta$ *cemK*, *bfrK* sequence, KF306078, *cemK* sequence, KF306079.

## 243 **Results**

### 244 ***In silico* prediction of the genetic loci *bfrKRT* and *cemAKR***

245 Inactivation of the gene *bfrK* (*lr70430*) impairs the ecological fitness of *L. reuteri*  
246 100-23 in the intestinal tract of mice (Frese *et al.*, 2011) but the function of the

247 *bfrKRT* operon remains unclear. The two-component system *bfrKRT* was  
248 predicted to be a peptide-based quorum sensing two-component regulatory system.  
249 Analysis also identified *cemAKR*, a two-component system with high sequence  
250 homology to *bfrKRT* (Fig. 1). The *bfrKRT* operon consists of genes coding for a  
251 putative histidine kinase of the HPK<sub>10</sub> subfamily, a response regulator of the  
252 LytR/AlgR family, and an ATP-binding cassette-type transporter with a  
253 bacteriocin processing peptidase C39 domain (Fig. 1). The *cemAKR* operon is  
254 composed of genes coding for an autoinducing peptide containing a conserved  
255 double-glycine (GG) motif in the leader peptide region, a histidine kinase of the  
256 HPK<sub>10</sub> subfamily, and a response regulator of the LytR/AlgR family (Fig. 1). The  
257 BAGEL program identified the putative signal transduction peptide IYSLLSL as  
258 *cemA* in *L. reuteri* 100-23. The nucleotide sequences of *bfrK* and *cemK* are very  
259 similar, as are *bfrR* and *cemR* (Fig. 1). *BfrKR* and *cemKR* are similar to the  
260 bacteriocin-related two-component system *abpKR* in *Lactobacillus salivarius*  
261 UCC118; *bfrT* is similar to *abpT* coding for the cognate bacteriocin export  
262 accessory protein in *Lactobacillus salivarius* UCC118 (KEGG database). The  
263 complementary genetic organization of the two operons implies a co-operation of  
264 the *bfrKRT* and *cemAKR* operons. The response regulator *cemR* was compared to  
265 other members of the LytR/AlgR family by BLASTP analysis and MUSCLE  
266 alignment. *CemR* was similar to *AgrA* (Peng *et al.*, 1988), *SppR* (Brurberg *et al.*,  
267 1997), *PlnC* (Diep *et al.*, 1996), *LamR*, (Fujii *et al.*, 2008), *ComE* (Ween *et al.*,  
268 2002), and *LytR* (Brunskill & Bayles, 1996; Kuroda *et al.*, 2001) (Table S1 of the

269 online supplementary material), suggesting that CemR functions as a response  
270 regulator controlled by an autoinducing peptide.

271 **Generation of *L. reuteri* single-gene and double-gene deletion mutants and**  
272 **the characterization of *bfrKRT* and *cemAKR* operons**

273 To determine whether there is cooperative regulation between the *bfrKRT* and  
274 *cemAKR* operons, the single-gene deletion mutants  $\Delta bfrK$ ,  $\Delta bfrR$ ,  $\Delta cemA$ , and  
275  $\Delta cemK$ , as well as the double-gene deletion mutants  $\Delta bfrK\Delta bfrR$ ,  $\Delta cemK\Delta cemR$ ,  
276  $\Delta bfrK\Delta cemK$ , and  $\Delta bfrR\Delta cemK$  (Table 1), were generated using site-specific  
277 homologous recombination mutagenesis and verified by PCR and DNA  
278 sequencing (Table S2 and S3). Physiological properties of the resulting *L. reuteri*  
279 mutant strains were characterized by observation of cell morphology and colony  
280 morphology, determination of autoaggregation, membrane fluidity and autolysis,  
281 and by observation of growth in a diverse set of adverse environmental conditions  
282 (Table S4). The disruption of genes in the *bfrKRT* and / or the *cemAKR* operons  
283 did not alter morphological characteristics of cells or colonies, aggregation,  
284 autolysis, membrane fluidity, or growth at low pH, high osmotic pressure, or in  
285 the presence of membrane-active inhibitors (Table S4).

286 **Cell adherence characteristics of *L. reuteri* wild type and mutant strains**

287 Some response regulators of the LytR/AlgR family regulate biofilm formation  
288 (Galperin, 2008). Therefore, the ability of *L. reuteri* 100-23 and its mutant strains  
289 to form biofilms was evaluated in two *in vitro* adherence assays. *L. reuteri*  
290 TMW1.106, a strain for which biofilm formation was previously characterized *in*

291 *vitro* and *in vivo*, was used for comparison (Walter *et al.*, 2008). Scanning  
292 electron microscopy was used to visualize the structure biofilms grown in  
293 presence of glucose or sucrose (Fig. 2). In sucMRS, *L. reuteri* 100-23 and 100-  
294 23 $\Delta$ *cemK* $\Delta$ *cemR* formed thick, stack-structured biofilms [Fig. 2(a, c)]. Biofilm  
295 formation was also observed with *L. reuteri* TMW1.106 (Fig. 2e). However, *L.*  
296 *reuteri* TMW1.106 $\Delta$ *gtfA* failed to form biofilms, owing to the disruption of  
297 reuteransucrase, which produces extracellular glucan as biofilm matrix (Walter *et*  
298 *al.*, 2008, Fig. 2g). In gluMRS, *L. reuteri* 100-23 did not form a biofilm (Fig. 2b),  
299 while *L. reuteri*  $\Delta$ *cemK* $\Delta$ *cemR* developed highly complex layers of biofilm (Fig.  
300 2d). Biofilms formed by *L. reuteri* TMW1.106 in gluMRS (Fig. 2f) were more  
301 dense when compared to *L. reuteri* TMW1.106 $\Delta$ *gtfA* (Fig. 2h). These results  
302 indicate that mechanisms of biofilm formation in *L. reuteri* are strain specific, and  
303 specific for different carbon sources. The *cemAKR* operon appears to regulate  
304 glucose-dependent biofilm formation in *L. reuteri* 100-23.

305 The microscopic observation of biofilm formation was verified by a quantitative  
306 assay (Fig. 3). Consistent with the microscopic observation, *L. reuteri* TMW1.106  
307 formed biofilms in gluMRS or sucMRS but *L. reuteri* TMW1.106 $\Delta$ *gtfA* was  
308 unable to form biofilm in either medium (Fig. 3). When grown in presence of  
309 sucrose, *L. reuteri* 100-23 and all mutants except *L. reuteri* 100-23 $\Delta$ *bfrK* $\Delta$ *cemK*  
310 formed biofilms (Fig. 3a). Cell densities of *L. reuteri* 100-23 $\Delta$ *bfrR*, 100-  
311 23 $\Delta$ *bfrK* $\Delta$ *bfrR*, 100-23 $\Delta$ *cemA*, and 100-23 $\Delta$ *bfrR* $\Delta$ *cemK* were higher when  
312 compared to *L. reuteri* 100-23. The density of cells of *L. reuteri* 100-23 adhering  
313 to the Petri dishes after growth in gluMRS was reduced in comparison to cells

314 after growth in sucMRS (Fig 3). When growing with glucose as carbon source,  
315 the adherence of all strains with mutations in *bfrR* or the *cemAKR* operon was  
316 higher when compared to the *L. reuteri* 100-23 and the cell densities were highest  
317 in strains with a mutation of *cemK* operon. The results of the quantitative  
318 determination of adherence and biofilm formation thus confirm that *cemAKR*  
319 regulates biofilm formation in the presence of glucose.

320 **Interaction between of *bfrKRT* and *cemAKR* regulons: analysis of gene**  
321 **expression by quantitative RT-PCR**

322 The expression of genes in the *bfrKRT* and *cemAKR* operons was determined by  
323 quantitative PCR to determine whether these two highly homologous two-  
324 component systems interact (Fig. 4). Expression of *bfrK* was unaffected by  
325 disruption of any other gene in the two operons; the expression of *bfrR* was  
326 significantly increased only by disruption of *bfrK* (Fig. 4). The transcription of  
327 *bfrT* increased in strains  $\Delta bfrK$  and  $\Delta bfrK\Delta bfrR$  and decreased in strain  $\Delta bfrR$  but  
328 remained unaffected by disruption of any of the genes in the *cemAKR* operon (Fig.  
329 4). In contrast, the expression of genes in the *cemAKR* operon was influenced by  
330 the *bfrKRT* operon. The expression of *cemK* was increased by disruption of *bfrK*  
331 and decreased by disruption of both *bfrK* and *bfrR*. The expression of *cemR* was  
332 significantly altered by disruption of *bfrK*, *cemA*, or *cemK*. The influence of BfrK  
333 on the expression of CemK and CemR implies interaction between these two two-  
334 component systems.

335 Since the *cemAKR* operon seems to play a role in the downstream signaling  
336 cascade, the *L. reuteri*  $\Delta cemK\Delta cemR$  strain was examined by qPCR to investigate



337 the influence of gene disruption on the expression of genes that relate to the  
338 production of autoinducing peptides, adhesion, biofilm dispersal, or  
339 exopolysaccharide production (Table 2). Genes involved in cyclopropane  
340 synthesis (*lr70615*), carbohydrate metabolism (*lr70618* and *lr71258*), and a cell  
341 division regulator (*lr71258*) were also included in the screening. Gene *lr70674*  
342 was included because it was incorrectly annotated as a mucus-binding protein. Of  
343 these genes, only the expression of *cemA* and *lr70674* was significantly different  
344 in *L. reuteri*  $\Delta$ *cemK* $\Delta$ *cemR* when compared to the wild-type strain (relative  
345 expression  $0.76 \pm 0.08$  and  $0.66 \pm 0.14$ , respectively). This result indicates that  
346 *cemA* is controlled by CemK and CemR. Gene *lr70674* encodes an  
347 osmoprotectant binding protein related to glycine betaine transport. However,  
348 tolerance of *L. reuteri*  $\Delta$ *cemK* $\Delta$ *cemR* to osmotic stress was not different when  
349 compared to the wild type strain (Supplementary Table S4).

## 350 **Discussion**

351 This study characterized the two-component regulatory systems *bfrKRT* and  
352 *cemAKR* operons, and assessed their influence on the physiology and biofilm  
353 formation of *L. reuteri* 100-23. The function of genes and their role in the two-  
354 component regulatory systems were deduced by comparison of isogenic knockout  
355 mutant strains with gene disruptions in one or two genes. Moreover, the  
356 hierarchical structure of the TCS signaling cascade was assessed based on the  
357 differential gene expressions of single-gene and double-gene knockout mutants.  
358 In most previous studies of *L. reuteri*, gene disruption was achieved by plasmid  
359 integration (Hung *et al.*, 2005; Schwab *et al.*, 2007; Walter *et al.*, 2008). With

360 these methods, a plasmid-borne antibiotic-resistance gene cassette remains in the  
361 chromosome of the mutant strain and limits the subsequent inactivation of other  
362 genes of interest. Single-stranded DNA recombineering (Van Pijkeren *et al.*,  
363 2012) or site-specific homologous recombination (Su *et al.*, 2011) are alternative  
364 approaches that were recently employed for genetic modification of *L. reuteri*.  
365 The multiple-deletion method employed in this study allowed the generation of  
366 double-gene knockout mutants.

367 Two-component regulatory systems are essential mechanisms in biofilm  
368 formation by *Streptococcus mutans* and *Staphylococcus aureus*. Two component  
369 systems known to regulate biofilm formation include the *comCDE* system of *S.*  
370 *mutans* (Senadheera & Cvitkovitch, 2008) and the *agrBDCA* system of *S. aureus*  
371 (Boles & Horswill, 2008). In these two systems, the response regulators ComE  
372 and AgrA were categorized as LytR/AlgR family proteins. Both are controlled by  
373 an autoinducing peptide (Nikolskaya & Galperin, 2002). Functions of regulatory  
374 proteins in the LytR/AlgR family include the regulation of virulence factors and  
375 in the performance of housekeeping functions, such as cell envelope maintenance,  
376 competence, and biofilm formation (Galperin, 2008). The response regulators  
377 BfrR and CemR investigated in this study are very similar to response regulation  
378 in the LytR/AlgR family (Table S1) and likely are controlled by the autoinducing  
379 peptide encoded by *cemA*.

380 The genetic organization of *bfrKRT* and *cemAKR* implies cooperative  
381 regulation between these two paralogous operons, which involves the sharing of  
382 the autoinducing peptide CemaA and the ABC transporter BfrT. The *cemAKR*

383 operon harbors an autoinducing peptide with a double-glycine (GG) type leader  
384 peptide, but lacks the corresponding ABC transporter. The *bfrKRT* operon in turn  
385 harbors an ABC transporter with a peptidase C39 domain that recognizes the GG-  
386 leader peptide. Moreover, nucleotide sequences of *bfrK* and *cemK* are 83%  
387 similar and the sequences of *bfrR* and *cemR* are 75% similar. These two operons  
388 thus may work cooperatively, similar to the Agr-like TCSs in *L. plantarum* and  
389 CpxA-CpxR and EnvZ-OmpR in *E. coli* (Bijlsma & Groisman, 2003; Fujii *et al.*,  
390 2008; Siryaporn & Goulian, 2008). Quantification of gene expression in *L. reuteri*  
391 100-23 and its knockout mutants demonstrated that disruption of *bfrK* altered the  
392 expression of *cemK* and *cemR*. Disruption of genes in the *cemAKR* operon,  
393 however, did not alter the expression of the genes in the *bfrKRT* operon. This  
394 result indicates that BrfK has the highest place in the hierarchy in a signaling  
395 cascade that also includes proteins encoded by *cemAKR*.

396 *L. reuteri* 100-23 mutants with disruptions in the *bfrKRT* and / or the  
397 *cemAKR* operons were assessed with respect to a comprehensive set of  
398 phenotypic characteristics. This evaluation identified adherence associated with  
399 biofilm formation as their only phenotype distinguishing these mutants from the  
400 wild type. *L. reuteri* 100-23 attaches and forms dense layers of cells on the non-  
401 secretory stratified squamous epithelium of the murine forestomach where the  
402 glucose concentration is 10 – 20 g (kg dry weight)<sup>-1</sup> (Schwab, 2006; Walter *et al.*,  
403 2008). Although the sucrose concentration in the forestomach of mice is much  
404 lower, sucrose metabolism and sucrose-dependent biofilm formation by *L. reuteri*  
405 100-23 has been demonstrated *in vivo* (Schwab, 2006; Sims *et al.*, 2011). *L.*

406 *reuteri* TMW1.106 produces exopolysaccharide (reuteran) from sucrose with an  
407 extracellular reuteransucrase (Schwab *et al.*, 2007). Disruption of the genes  
408 coding for reuteransucrases and fructansucrases in *L. reuteri* reduced the  
409 competitiveness of mutant strains in the forestomach of mice in competition with  
410 the corresponding wild type strains but mutant strains colonized mice when  
411 administered in pure culture (Walter *et al.*, 2008; Sims *et al.*, 2011). However,  
412 disruption of the reuteransucrase producing the extracellular biofilm matrix could  
413 be complemented by co-colonization of a reuteran-producing wild type strain  
414 (Walter *et al.*, 2008). The *in vitro* biofilm formation is a simplified model system  
415 for the *in vivo* situation because it uses an abiotic support, a constant carbon  
416 supply (sucrose or glucose), and because competing microbiota are absent.  
417 However, the *in vitro* biofilm formation and coaggregation by *L. reuteri*  
418 TMW1.106, LTH5448 and 100-23 generally corresponded to competitiveness and  
419 biofilm formation *in vivo* (Walter *et al.*, 2008, Sims *et al.*, 2011, Frese *et al.*, 2011;  
420 this study).

421         Although the formation of biofilms by *L. reuteri* 100-23 and TMW1.106  
422 *in vitro* and *in vivo* is supported by sucrose, the mechanisms of biofilm formations  
423 exhibit strain specific differences. *L. reuteri* TMW1.106 but not 100-23 employs  
424 an extracellular reuteransucrase to synthesise the biofilm matrix (Schwab *et al.*,  
425 2007; Sims *et al.*, 2011; Walter *et al.*, 2008). Analysis of the genetic locus of  
426 *bfrKRT* in *L. reuteri* 100-23 identified two IS elements upstream and downstream  
427 of *bfrKRT*. The presence of *bfrKRT* in the rodent lineage strains of *L. reuteri* is  
428 variable but the operon is rodent specific (Frese *et al.*, 2011). It is likely that the

429 *bfrKRT* operon results of lateral gene transfer in a manner similar to that of  
430 fructansucrase (*ftf*) in *L. reuteri* 100-23 (Sims *et al.*, 2011) and allows *L. reuteri* to  
431 adapt to different environments.

432         The quantitative assessment of biofilm formation that was performed in  
433 this study indicated that *L. reuteri* 100-23 formed less dense biofilm with glucose  
434 as sole carbon source when compared to *L. reuteri* TMW1.106. With glucose as  
435 the sole carbon source, biofilm formation of *L. reuteri* 100-23 was repressed by  
436 proteins coded by the *cemAKR* operon. *BfrK* is overexpressed by *L. reuteri* 100-  
437 23 during colonization of the murine forestomach epithelium (Frese *et al.*, 2013)  
438 and disruption of *bfrK* impaired *in vivo* colonization of mice (Frese *et al.*, 2011).  
439 However, disruption of *bfrK* did not reduce *in vivo* biofilm formation, suggesting  
440 that the gene may be functionally redundant (Frese *et al.*, 2013). This study  
441 confirmed and extended the *in vivo* results by demonstration that *bfrK* did not  
442 substantially alter adherence and biofilm formation ability of *L. reuteri* 100-23  
443 with sucrose or glucose as carbon source (this study). Moreover, cooperative gene  
444 regulation through the *bfrKRT* and *cemAKR* operons may account for a partial  
445 overlap of the functions of the histidine kinases BfrK and CemK.

446 *L. reuteri* has adapted to specific vertebrate hosts. This adaptation allowed the  
447 identification of genetic or metabolic traits that are required for colonization of  
448 intestinal ecosystems. Genetic traits of *L. reuteri* contribute to biofilm formation  
449 and the ecological fitness in rodents were recently reviewed (Frese *et al.*, 2013;  
450 Frese *et al.*, 2011; Walter, 2008) and are depicted in Figure 5. Biofilm formation  
451 contributes to the competitiveness of *L. reuteri* in intestinal ecosystems. However,

452 the proteins that are involved in attachment and biofilm formation by *L. reuteri*  
453 are strain-specific and have not been fully elucidated (Frese *et al.*, 2011; Walter *et*  
454 *al.*, 2008). Attachment of *L. reuteri* to intestinal epithelia is mediated by the large  
455 surface protein coded by *lsp* (Walter *et al.*, 2005), the mucus adhesion-promoting  
456 protein MapA or the mucus-binding protein Mub (Miyoshi *et al.*, 2006; Roos &  
457 Jonsson, 2002). The D-alanine-D-ananyl carrier protein ligase (DltA) also affects  
458 the ability of *L. reuteri* ability to adhere and to resist acid stress (Walter *et al.*,  
459 2007). The present study demonstrated that disruption of *bfrKRT* enhanced  
460 sucrose-dependent biofilm formation of *L. reuteri* 100-23, and altered expression  
461 of the *cemAKR* operon (Fig. 5). Disruption of genes in the *cemAKR* operon  
462 enhanced glucose-dependent biofilm formation. Unlike the the *comCDE* system  
463 of *S. mutans* and the *agrBDCA* system of *S. aureus*, the *bfrKRT* and *cemAKR*  
464 systems of *L. reuteri* 100-23 did not influence the expression of genes encoding  
465 exopolysaccharide formation, biofilm dispersal (the *lytSR* system and the *lrg*  
466 operon), or another quorum-sensing autoinducing peptide and ABC transporter  
467 (*lr70531*, *lr70532*). Data presented in this study link the *bfrKRT* and *cemAKR*  
468 systems of *L. reuteri* to biofilm formation.

469 In conclusion, this study characterized several single and multiple deletion  
470 mutants to characterize the two-component systems *bfrKRT* and *cemAKR* in *L.*  
471 *reuteri* 100-23. Deletion of the histidine kinase BfrK impairs ecological fitness of  
472 *L. reuteri* 100-23 in mice but the function of the operons remained unknown  
473 (Frese *et al.*, 2011). Deletion of single or multiple genes in the operons *bfrKRT*  
474 and *cemAKR* did not affect cell morphology, growth rate, or the sensitivity to

475 various stressors. However, several mutants exhibited increased adherence and  
476 biofilm formation *in vitro*. The effect of gene disruption on adherence and biofilm  
477 formation was dependent on the carbon source. Moreover, quantification of gene  
478 expression indicated cross talk between these two operons. The study thus links  
479 the contribution of *bfrK* on the competitiveness of *L. reuteri in vivo* to biofilm  
480 formation and adherence to the forestomach epithelium. However, the genes  
481 required for formation of the extracellular biofilm matrix in *L. reuteri* 100-23  
482 remain unknown. The networks regulating of biofilm formation by *L. reuteri* and  
483 the specific contribution of the *bfrKRT* and *cemAKR* operons to biofilm formation  
484 *in vitro* and *in vivo* thus remain to be elucidated.

#### 485 **Acknowledgements**

486 We are grateful to Jens Walter for helpful discussions and critical review of the  
487 manuscript, and appreciate the technical support from Troy Locke and Arlene  
488 Oatway with the qPCR analysis and scanning electron microscopy. The National  
489 Science and Engineering Council of Canada provided financial support; M.  
490 Gänzle acknowledges the Canada Research Chairs program for funding.

#### 491 **References**

492 **Bairoch, A., Apweiler, R., Wu, C. H., Barker, W. C., Boeckmann, B.,**  
493 **Ferro, S., Gasteiger, E., Huang, H., Lopez, R. & other authors (2005).** The  
494 Universal Protein Resource (UniProt). *Nucleic Acids Res* **33**, D154–159.

495 **Bijlsma, J. J. & Groisman, E. A. (2003).** Making informed decisions:  
496 regulatory interactions between two-component systems. *Trends Microbiol*  
497 **11**, 359–366.

498 **Boles, B. R. & Horswill, A. R. (2008).** *agr*-mediated dispersal of  
499 *Staphylococcus aureus* biofilms. *PLoS Pathog* **4**, e1000052.

500 **Brunskill, E. W. & Bayles, K. W. (1996).** Identification and molecular  
501 characterization of a putative regulatory locus that affects autolysis in  
502 *Staphylococcus aureus*. *J Bacteriol* **178**, 611–618.

503 **Brurberg, M. B., Nes, I. F. & Eijsink, V. G. (1997).** Pheromone-induced  
504 production of antimicrobial peptides in *Lactobacillus*. *Mol Microbiol* **26**, 347–  
505 360.

506 **de Jong, A., van Hijum, S. A., Bijlsma, J. J., Kok, J. & Kuipers, O. P.**  
507 **(2006).** BAGEL: a web-based bacteriocin genome mining tool. *Nucleic Acids*  
508 *Res* **34**, W273–279.

509 **Diep, D. B., Håvarstein, L. S. & Nes, I. F. (1996).** Characterization of the  
510 locus responsible for the bacteriocin production in *Lactobacillus plantarum*  
511 C11. *J Bacteriol* **178**, 4472–4483.

512 **Frese, S. A., Benson, A. K., Tannock, G. W., Loach, D. M., Kim, J.,**  
513 **Zhang, M., Oh, P. L., Heng, N. C., Patil, P. B. and other authors (2011).**  
514 The evolution of host specialization in the vertebrate gut symbiont  
515 *Lactobacillus reuteri*. *PLoS Genet* **7**, e1001314.



516 **Frese, S.A., MacKenzie, D.A., Peterosn, D.A., Schmaltz, R., Fangman, T.,**  
517 **Zhou, Y., Chang, C., Benson, A.K., cody, L.A., and other authors. (2013).**  
518 Molecular characterization of host-specific biofilm formation in a vertebrate  
519 gut symbiont. *PLoS Genet* 9, e1004057.

520 **Fujii, T., Ingham, C., Nakayama, J., Beerthuyzen, M., Kunuki, R.,**  
521 **Molenaar, D., Sturme, M., Vaughan, E., Kleerebezem, M. & de Vos, W.**  
522 **(2008).** Two homologous Agr-like quorum-sensing systems cooperatively  
523 control adherence, cell morphology, and cell viability properties in  
524 *Lactobacillus plantarum* WCFS1. *J Bacteriol* **190**, 7655–7665.

525 **Fuller, R, Barrow, P.A., & Brooker, B. E. (1978)** Bacteria associated with  
526 the gastric epithelium of neonatal pigs. *Appl Environm Microbiol* **35**: 582-591.

527 **Fuller, R. (1973)** Ecological studies on the *Lactobacillus* flora associated  
528 with the crop epithelium of the fowl. *J. Appl. Bact.* **36**:131-139.

529 **Fuller, R., and Brooker, B.E. (1974)** Lactobacilli which attach to the crop  
530 epithelium of the fowl. *Am J Clin Nutr* **27**: 1305–1312.

531 **Galperin, M. Y. (2008).** Telling bacteria: do not LytTR. *Structure* **16**, 657–  
532 659.

533 **Gänzle, M. G., Holtzel, A., Walter, J., Jung, G. & Hammes, W. P. (2000).**  
534 Characterization of reutericyclin produced by *Lactobacillus reuteri* LTH2584.  
535 *Appl Environ Microbiol* **66**, 4325–4333.

536 **Hung, J., Turner, M. S., Walsh, T. & Giffard, P. M. (2005).** BspA (CyuC)  
537 in *Lactobacillus fermentum* BR11 is a highly expressed high-affinity L-  
538 cystine-binding protein. *Curr Microbiol* **50**, 33–37.

539 **Karatan, E. & Watnick, P. (2009).** Signals, regulatory networks, and  
540 materials that build and break bacterial biofilms. *Microbiol Mol Biol Rev* **73**,  
541 310–347.

542 **Kuroda, M., Ohta, T., Uchiyama, I., Baba, T., Yuzawa, H., Kobayashi, I.,**  
543 **Cui, L., Oguchi, A., Aoki, K. & other authors (2001).** Whole genome  
544 sequencing of methicillin-resistant *Staphylococcus aureus*. *Lancet* **357**, 1225–  
545 1240.

546 **Loo, C. Y., Corliss, D. A. & Ganeshkumar, N. (2000).** *Streptococcus*  
547 *gordonii* biofilm formation: identification of genes that code for biofilm  
548 phenotypes. *J Bacteriol* **182**, 1374–1382.

549 **Mitrophanov, A. Y. & Groisman, E. A. (2008).** Signal integration in  
550 bacterial two-component regulatory systems. *Genes Dev* **22**, 2601–2611.

551 **Miyoshi, Y., Okada, S., Uchimura, T. & Satoh, E. (2006).** A mucus  
552 adhesion promoting protein, MapA, mediates the adhesion of *Lactobacillus*  
553 *reuteri* to Caco-2 human intestinal epithelial cells. *Biosci Biotechnol Biochem*  
554 **70**, 1622–1628.

555 **Nikolskaya, A. N. & Galperin, M. Y. (2002).** A novel type of conserved  
556 DNA-binding domain in the transcriptional regulators of the AlgR/AgrA/LytR  
557 family. *Nucleic Acids Res* **30**, 2453–2459.

558 **Nobbs, A. H., Lamont, R. J. & Jenkinson, H. F. (2009).** *Streptococcus*  
559 adherence and colonization. *Microbiol Mol Biol Rev* **73**, 407–450.

560 **Peng, H. L., Novick, R. P., Kreiswirth, B., Kornblum, J. & Schlievert, P.**  
561 **(1988).** Cloning, characterization, and sequencing of an accessory gene  
562 regulator (*agr*) in *Staphylococcus aureus*. *J Bacteriol* **170**, 4365–4372.

563 **Perez-Casal, J., Price, J. A., Maguin, E. & Scott, J. R. (1993).** An M  
564 protein with a single C repeat prevents phagocytosis of *Streptococcus*  
565 *pyogenes*: use of a temperature-sensitive shuttle vector to deliver homologous  
566 sequences to the chromosome of *S. pyogenes*. *Mol Microbiol* **8**, 809–819.

567 **Pfaffl, M. W. (2001).** A new mathematical model for relative quantification  
568 in real-time RT-PCR. *Nucleic Acids Res* **29**, 2002–2007.

569 **Quivey, R. G., Kuhnert, W. L. & Hahn, K. (2001).** Genetics of acid  
570 adaptation in oral streptococci. *Crit Rev Oral Biol Med* **12**, 301–314.

571 **Roos, S. & Jonsson, H. (2002).** A high-molecular-mass cell-surface protein  
572 from *Lactobacillus reuteri* 1063 adheres to mucus components. *Microbiology*  
573 **148**, 433–442.

574 **Savage, D.C., Dubos, R., and Schaedler, R.W. (1968).** The gastrointestinal  
575 epithelium and its autochthonous bacterial flora. *J Exp Med* **127**: 67–76.

576 **Schwab, C. (2006).** Regulation and ecological relevance of  
577 fructosyltransferases in *Lactobacillus reuteri*. Doctoral thesis, Center of Life  
578 Sciences Weihenstephan, TU Munich.

579 **Schwab, C., Walter, J., Tannock, G. W., Vogel, R. F. & Gänzle, M. G.**  
580 **(2007).** Sucrose utilization and impact of sucrose on glycosyltransferase  
581 expression in *Lactobacillus reuteri*. *System Appl Microbiol* **30**, 433–443.

582 **Senadheera, D. & Cvitkovitch, D. G. (2008).** Quorum sensing and biofilm  
583 formation by *Streptococcus mutans*. *Adv Exp Med Biol* **631**, 178–188.

584 **Senadheera, M. D., Lee, A. W., Hung, D. C., Spatafora, G. A., Goodman,**  
585 **S. D. & Cvitkovitch, D. G. (2007).** The *Streptococcus mutans vicX* gene  
586 product modulates *gtfB/C* expression, biofilm formation, genetic competence,  
587 and oxidative stress tolerance. *J Bacteriol* **189**, 1451–1458.

588 **Sims, I. M., Frese, S. A., Walter, J., Loach, D., Wilson, M., Appleyard, K.,**  
589 **Eason, J., Livingston, M., Baird, M. & other authors (2011).** Structure and  
590 functions of exopolysaccharide produced by gut commensal *Lactobacillus*  
591 *reuteri* 100-23. *ISME J* **5**, 1115–1124.

592 **Siryaporn, A. & Goulian, M. (2008).** Cross-talk suppression between the  
593 CpxA-CpxR and EnvZ-OmpR two-component systems in *E. coli*. *Mol*  
594 *Microbiol* **70**, 494–506.

595 **Su, M. S., Oh, P. L., Walter, J. & Gänzle, M. G. (2012).** Intestinal origin of  
596 sourdough *Lactobacillus reuteri* isolates as revealed by phylogenetic, genetic,  
597 and physiological analysis. *Appl Environ Microbiol* **78**, 6777–6780.

598 **Su, M. S., Schlicht, S. & Gänzle, M. G. (2011).** Contribution of glutamate  
599 decarboxylase in *Lactobacillus reuteri* to acid resistance and persistence in  
600 sourdough fermentation. *Microbial Cell Factories* **10** (Suppl 1), S8.

601 **Van Pijkeren, J. P., Neoh, K. M., Sirias, D., Findley, A. S. & Britton, R. A.**  
602 **(2012).** Exploring optimization parameters to increase ssDNA recombineering  
603 in *Lactococcus lactis* and *Lactobacillus reuteri*. *Bioengineered* **3**, 209–217.

604 **Vogel, R. F., Knorr, R., Müller, M. R., Steudel, U., Gänzle, M. G. &**  
605 **Ehrmann, M. A. (1999).** Non-dairy lactic fermentations: the cereal world.  
606 *Antonie Van Leeuwenhoek* **76**, 403–411.

607 **Walter, J. (2008).** Ecological role of lactobacilli in the gastrointestinal tract:  
608 implications for fundamental and biomedical research. *Appl Environ*  
609 *Microbiol* **74**, 4985–4996.

610 **Walter, J., Britton, R. A. & Roos, S. (2011).** Host-microbial symbiosis in  
611 the vertebrate gastrointestinal tract and the *Lactobacillus reuteri* paradigm.  
612 *Proc Natl Acad Sci U S A* **108**, 4645–4652.

613 **Walter, J., Chagnaud, P., Tannock, G. W., Loach, D. M., Dal Bello, F.,**  
614 **Jenkinson, H. F., Hammes, W. P. & Hertel, C. (2005).** A high-molecular-  
615 mass surface protein (Lsp) and methionine sulfoxide reductase B (MsrB)

616 contribute to the ecological performance of *Lactobacillus reuteri* in the  
617 murine gut. *Appl Environ Microbiol* **71**, 979–986.

618 **Walter, J., Loach, D. M., Alqumber, M., Rockel, C., Hermann, C.,**  
619 **Pfitzenmaier, M. & Tannock, G. W. (2007).** D-alanyl ester depletion of  
620 teichoic acids in *Lactobacillus reuteri* 100-23 results in impaired colonization  
621 of the mouse gastrointestinal tract. *Environ Microbiol* **9**, 1750–1760.

622 **Walter, J., Schwab, C., Loach, D. M., Gänzle, M. G. & Tannock, G. W.**  
623 **(2008).** Glucosyltransferase A (GtfA) and inulosucrase (Inu) of *Lactobacillus*  
624 *reuteri* TMW1.106 contribute to cell aggregation, in vitro biofilm formation,  
625 and colonization of the mouse gastrointestinal tract. *Microbiology* **154**, 72–80.

626 **Ween, O., Teigen, S., Gaustad, P., Kilian, M. & Håvarstein, L. S. (2002).**  
627 Competence without a competence pheromone in a natural isolate of  
628 *Streptococcus infantis*, *J Bacteriol* **184**, 3426–3432.

629 **Wesney, E. & Tannock, G. W. (1979).** Association of rat, pig and fowl  
630 biotypes of lactobacilli with the stomach of gnotobiotic mice. *Microb Ecol* **5**,  
631 35–42.

632 **Wilson, C. M., Aggio, R. B. M., O'Toole, P. W., Villas-Boas, S. &**  
633 **Tannock, G. W. (2012).** Transcriptional and metabolomic consequences of  
634 *luxS* inactivation reveal a metabolic rather than quorum-sensing role for LuxS  
635 in *Lactobacillus reuteri* 100-23. *J Bacteriol* **194**, 1743–1746.

636 **Yuki, N., Shimazaki, T., Kushiro, A, Watanabe, K., Uchida, K., Yuyama,**  
637 **T, & Morotomi, M. (2000)** Colonization of the stratified squamous  
638 epithelium of the nonsecreting area of horse stomach by lactobacilli. *Appl*  
639 *Environm Microbiol* **66**: 5030–5034.

640 **Zhang, Z. G., Ye, Z. Q., Yu, L. & Shi, P. (2011).** Phylogenomic  
641 reconstruction of lactic acid bacteria: an update. *BMC Evol Biol* **11**, 1–12

642 **Figure legends:**

643 **Figure 1.** Schematic representation of the two-component regulatory systems *bfrKRT* and  
644 *cemAKR* operons and their protein sequence analysis. Bioinformatic analysis of histidine  
645 kinases BfrK and CemK reveals an amino-terminal transmembrane domain and a carboxyl  
646 terminal ATPase-like ATP-binding domain, where the specific homology boxes H, X, N,  
647 and G assign features to the HPK<sub>10</sub> subfamily. The functional domains of response  
648 regulators BfrR and CemR are predicted as CheY-like superfamily receiver with conserved  
649 aspartate (D) and lysine (K) residues at the amino-terminus, along with LytTR DNA-  
650 binding domain of the LytR/AlgR family at the carboxyl-terminus. The functional  
651 prediction of BfrT shows a bacteriocin processing peptidase C39 domain, transmembrane  
652 segments, and ABC transporter-like domain. CemA was identified using the BAGEL  
653 program, which also revealed it was a bacteriocin-like autoinducing peptide, which  
654 contains a conserved double-glycine (GG) motif in the leader peptide region. Numbers  
655 indicate the protein identity of the histidine kinases and response regulators.

656 **Figure 2.** SEM micrographs of *L. reuteri* cells on polystyrene surfaces. *L. reuteri* 100-23  
657 (a, b),  $\Delta cemK\Delta cemR$  (c, d), TMW1.106 (e, f), and  $\Delta gtfA$  (g, h) were grown in MRS media  
658 containing either 2% sucrose (a, c, e, and g) or 2% glucose (b, d, f, and h). Micrographs  
659 were taken from six different fields of two independent experiments. Magnification is  $\times$   
660 5000.

661 **Figure 3.** Adherence ability of *L. reuteri* on polystyrene plates. Quantitative analysis of  
662 cells adhered to polystyrene plates was carried out using cells that were grown over 24 h,  
663 which were inoculated in MRS broth containing 2% sucrose (black bar, panel A) or 2%



664 glucose (grey bar, panel B). Adherence ability was measured by an optical density of 600  
665 nm. A significant difference between the adherence ability of the mutant strains and the  
666 wild-type strains is indicated by asterisk (\*) ( $p < 0.05$ ). Data shown are the means of three  
667 independent experiments with standard deviations.

668 **Figure 4.** Relative quantification of gene expression in *L. reuteri* 100-23 and its derived  
669 mutant strains grown in gluMRS. The expressions of the *bfrKRT* and *cemAKR* operons  
670 were determined by qPCR (the y-axis; linear scale) with primers specific to genes *bfrK*,  
671 *bfrR*, *bfrT*, *cemK* and *cemR* (the x-axis). The *L. reuteri* isogenic strains used in this study  
672 are  $\Delta bfrK$ ,  $\Delta bfrR$ ,  $\Delta bfrK\Delta bfrR$ ,  $\Delta cemA$ ,  $\Delta cemK$ ,  $\Delta cemK\Delta cemR$ ,  $\Delta bfrK\Delta cemK$ , and  
673  $\Delta bfrR\Delta cemK$ . A significant difference from the wild-type strain (relative gene expression =  
674 1) is indicated by asterisk (\*) ( $p < 0.05$ ). The results are shown as means  $\pm$  the standard  
675 deviations of three independent experiments performed in triplicate. Primers targeting  
676 deleted genes in mutant strains yielded no amplicons in RT-qPCR reactions; these controls  
677 are indicated by the letter “X”.

678 **Figure 5.** Schematic overview of the TCS regulatory signaling cascade of the *bfrKRT* and  
679 *cemAKR* operons, and its relationship to the genes related to ecological performance of  
680 *L. reuteri* in the intestinal tract of mice. Dashed lines indicate relationships that were  
681 established on the basis of quantification of gene expression. The TCS involves signal  
682 sensing by a histidine kinase (BfrK, CemK), followed by histidine (H) phosphorylation and  
683 phosphotransfer to an aspartate (D) of a response regulator (BfrR, CemR). Disruptions in  
684 *bfrKR* affect expression of *bfrT* as well as genes in the *cemAKR* operon when glucose is the  
685 sole carbohydrate source in the growth media; disruption of *cemRK* does not affect  
686 expression of *bfrKRT* but alters expression of *cemA* and *lr70674* (osmoprotectant binding

687 protein). Because a transport enzyme is not part of the *cemAKR* system, the maturation of  
688 the autoinducing peptide Cema may be processed and transported by the ABC transporter  
689 BfrT. Mutations in the *bfrKRT* system as well as *cemA* affected predominantly biofilm  
690 formation with sucrose as carbon source while disruption of genes in the *cemAKR* system  
691 has a stronger effect on glucose-dependent regulons of biofilm formation.

692 Adherence of *L. reuteri* to mouse epithelial cells is mediated by *lsp* (Walter *et al.*, 2005).  
693 The membrane protein D-alanine-D-ananyl carrier protein ligase (DltA) affects *L. reuteri*'s  
694 ability to adhere and to resist acid stress (Walter *et al.*, 2007). Extracellular glucansucrases  
695 and levansucrase contribute to biofilm formation *in vitro* and ecological fitness *in vivo*  
696 (Walter *et al.*, 2008). Disruption of the *secA2* operon and ABC transporters (*lr70458*,  
697 *lr70532*) also impaired colonization of mice by *L. reuteri* (Frese *et al.*, 2011).

698 Methionine-R-sulfoxide reductase, coded by *msrB* in *L. reuteri* 100-23, is an antioxidant  
699 repair enzyme reducing methionine sulfoxide to methionine. Disruption of *msrB* has  
700 impairs colonisation of mice by *L. reuteri* (Walter *et al.*, 2005). Disruption of *luxS* in *L.*  
701 *reuteri* 100-23 is associated with the metabolic conversion of S-ribosyl homocysteine to  
702 homocysteine but not AI-2 quorum-sensing regulation (Wilson *et al.*, 2012). Genes *gadB*  
703 (Su *et al.*, 2011) and *dltA* (Walter *et al.*, 2007) increase acid resistance of *L. reuteri*.

704

705 **Table 1.** Bacterial strains used in this study

Strains	Relevant genotype or description	Source or reference
<i>Escherichia coli</i> JM109	Cloning host for pGEMTeasy- and pJRS233-derived plasmids	Promega
<i>Lactobacillus reuteri</i>		
TMW1.106	Type II sourdough isolate; wild type strain producing glucan and fructan	Schwab et al. (2007)
TMW1.106 $\Delta$ <i>gtfA</i>	TMW1.106 $\Delta$ <i>gtfA</i> ::pORI28; non-glucan producing strain; Erm <sup>r</sup>	Walter <i>et al.</i> , (2008)
100-23	Rodent isolate; wild type strain producing levan	Wesney & Tannock (1979)
100-23 $\Delta$ <i>bfrK</i>	Truncation of <i>bfrK</i>	This study
100-23 $\Delta$ <i>bfrR</i>	Truncation of <i>bfrR</i>	This study
100-23 $\Delta$ <i>bfrK</i> $\Delta$ <i>bfrR</i>	Truncation of <i>bfrK</i> and <i>bfrR</i>	This study
100-23 $\Delta$ <i>cemA</i>	Truncation of <i>cemA</i>	This study
100-23 $\Delta$ <i>cemK</i>	Truncation of <i>cemK</i>	This study
100-23 $\Delta$ <i>cemK</i> $\Delta$ <i>cemR</i>	Truncation of <i>cemK</i> and <i>cemR</i>	This study
100-23 $\Delta$ <i>bfrK</i> $\Delta$ <i>cemK</i>	Truncation of <i>bfrK</i> and <i>cemK</i>	This study
100-23 $\Delta$ <i>bfrR</i> $\Delta$ <i>cemK</i>	Truncation of <i>bfrR</i> and <i>cemK</i>	This study

706 Erm<sup>r</sup>, erythromycin resistance gene

707 **Table 2.** Quantitative PCR primers used in this study

Primer name	Sequence (5' - 3')	Target gene's locus_tag	Features of putative protein
<i>recA</i> -qPCR-F2	CAACTATCCGGATGGAAATTCGTCG	Lreu23DRAFT_3582	RecA; endogenous protein; DNA recombination
<i>recA</i> -qPCR-R2	TGTCAACTTCACAACGTTTGAATGGC		
<i>bfrK</i> -qPCR-F1	CGGACTAGGCTATATTGGATCGTATT	Lreu23DRAFT_4807	BfrK; histidine kinase of the HPK <sub>10</sub> family; two-component system
<i>bfrK</i> -qPCR-R1	GTTGGATGCCCTTCGTTTGTA		
<i>bfrR</i> -qPCR-F2	CTCAGCAAATTCAAAAAAGCACCGT	Lreu23DRAFT_4808	BfrR; response regulator of the LytR/AlgR family; two-component system
<i>bfrR</i> -qPCR-R2	ATCGCCGTTGCAATTTTCGTTG		
<i>bfrT</i> -qPCR-F3	ACTAAAGCCTGCAAAGTTGCGATGAT	Lreu23DRAFT_4809	BfrT; ABC-type bacteriocin transporter; two-component system
<i>bfrT</i> -qPCR-R3	TTGTCCACCTGAAAGGGTAGTAGCATTTTC		
<i>cemK</i> -qPCR-F1	AGGACTTACTTTTGAACCTTTTCACATTCTT	Lreu23DRAFT_4825	CemK; histidine kinase of the HPK <sub>10</sub> family; two-component system
<i>cemK</i> -qPCR-R1	CATATTCCTTATGATTGGCTTAGGTTATAC		
<i>cemR</i> -qPCR-F2	CAGTCTAGCTTAATTAACCTACAAAATGTTGA	Lreu23DRAFT_4826	CemR; response regulator of the LytR/AlgR family; two-component system
<i>cemR</i> -qPCR-R2	CGGCTTATTAAGTTTTCCAACAATG		
<i>cemA</i> -qPCR-F2	TGATATATTTATGCAAAAACCTATCAATTCATC	N.D.	CemA; autoinducing peptide of peptide-based quorum sensing two-component system
<i>cemA</i> -qPCR-R2	TTATTTACAGACTTAAAAGTGAGTATATACCA CCC		
<i>lr69269</i> -qPCR762-F2	TGCAGTGAGTATCACCGATAGACA	Lreu23DRAFT_3257	LytS; histidine kinase; cell autolysis; two-component system
<i>lr69269</i> -qPCR836-R2	TTTCCTGGGATATGGTGATCATC		
<i>lr69270</i> -qPCR365-F2	AGGATGATGCTACCAAAGCTAAGAG	Lreu23DRAFT_3258	LytR; response regulator of the LytR/AlgR family; cell autolysis; two-component system
<i>lr69270</i> -qPCR-439-R2	TCGTTGCTCGTCATTTTGA		
<i>lr69271</i> -qPCR46-F2	ATGGGAATCTTTGCTGCAATTT	Lreu23DRAFT_3259	Putative negative effector of murein hydrolase LrgA; cell lysis; regulation of murein hydrolase activity
<i>lr69271</i> -qPCR120-R2	AGGAACAACGAAACTCTTAGGAAAAA		
<i>lr69272</i> -qPCR278-F2	CGCTTATCGCCGGAATG	Lreu23DRAFT_3260	Putative negative effector of murein hydrolase; LrgB-like holing/antiholin; cell lysis; regulation of murein hydrolase activity
<i>lr69272</i> -qPCR352-R2	TGAATCCACCCACAAATAATGTG		

**Table 2.** –continued- Quantitative PCR primers used in this study

Primer name	Sequence (5' - 3')	Target gene's locus_tag	Features of putative protein
<i>lr69363</i> -qPCR261-F1	GGATTCACTAATTGCCGGTCTT	Lreu23DRAFT_3339	Homolog of BspA/CyuC/MapA/CnBP
<i>lr69363</i> -qPCR336-R1	CCG TTCAGGTGTCTGTGTAATATTG		collagen binding protein; cystine transporter, amino acid ABC transporter substrate-binding protein, PAAT family; signal transduction systems, periplasmic component/ domain
<i>lr69863</i> -qPCR40-F4	AAGCAATGGATAACAGCTGCAA	Lreu23DRAFT_4288	Homolog of glucansucrase/ reuteransucrase;
<i>lr69863</i> -qPCR114-R4	AGCTTGTGCCACACCTCCTAAA		exopolysaccharide synthesis
<i>lr70531</i> -qPCR38-F1	AGGTTTCTGGTGGATGGAGTCTAT	Lreu23DRAFT_4899	Bacteriocin-type signal sequence; quorum sensing two-component system
<i>lr70531</i> -qPCR119-R1	TGAGCCCATTTGTTCAAGGAA		
<i>lr70532</i> -qPCR366-F1	TCGGGATGAATTTGGTCGTT	Lreu23DRAFT_4900	ABC-type bacteriocin transporter; quorum sensing two-component system
<i>lr70532</i> -qPCR440-R1	TTTTGTGGCGTATATCCCTTAGC		
<i>lr70615</i> -qPCR868-F2	GGCGGCTATGTACCTGGTCTT	Lreu23DRAFT_4979	Cyclopropane-fatty-acyl-phospholipid synthase; cyclopropane synthesis
<i>lr70615</i> -qPCR943-R2	TTTCGATATCAGCGATTTGCA		
<i>lr70618</i> -qPCR1234-F2	CTGTTAATTAGTAACGGGATGCAAAC	Lreu23DRAFT_4982	Acetolactate synthase, large subunit; carbohydrate metabolism
<i>lr70618</i> -qPCR1308-R2	GGGATAAAGCATCGCTGCAA		
<i>lr70674</i> -qPCR242-F1	GCGAAGTTGACGTTTATCCTGAT	Lreu23DRAFT_5027	Glycine betaine/choline-binding (lipo)protein of an ABC-type transport system; osmoprotectant binding protein
<i>lr70674</i> -qPCR316-R1	TCTTGCCAGTCCCCTTCTTTT		
<i>lr71010</i> -qPCR1242-F1	CACTCTTCGTGATGCTCATGTTATC	Lreu23DRAFT_3826	Large surface protein with LPXTG-motif cell wall anchor domain; homolog of FtfA/
<i>lr71010</i> -qPCR1317-R1	CGTTCCAGTGTTCCTCAA		levansucrase/ inulosucrase; exopolysaccharide synthesis
<i>lr71188</i> -qPCR259-F1	CCAAGGTTTTTGCGGGATT	Lreu23DRAFT_3689	Cell division-specific peptidoglycan biosynthesis regulator FtsW; cell division
<i>lr71188</i> -qPCR333-R1	AACAGCTCGGCTAAAGACTAAAACA		
<i>lr71258</i> -qPCR638-F1	CAATCACTGCCGTAAAGAATGGT	Lreu23DRAFT_3623	Acetate kinase; carbohydrate metabolism
<i>lr71258</i> -qPCR712-R1	CCATTGTTATTCCCGCAACAG		

708 N.D., not determined.

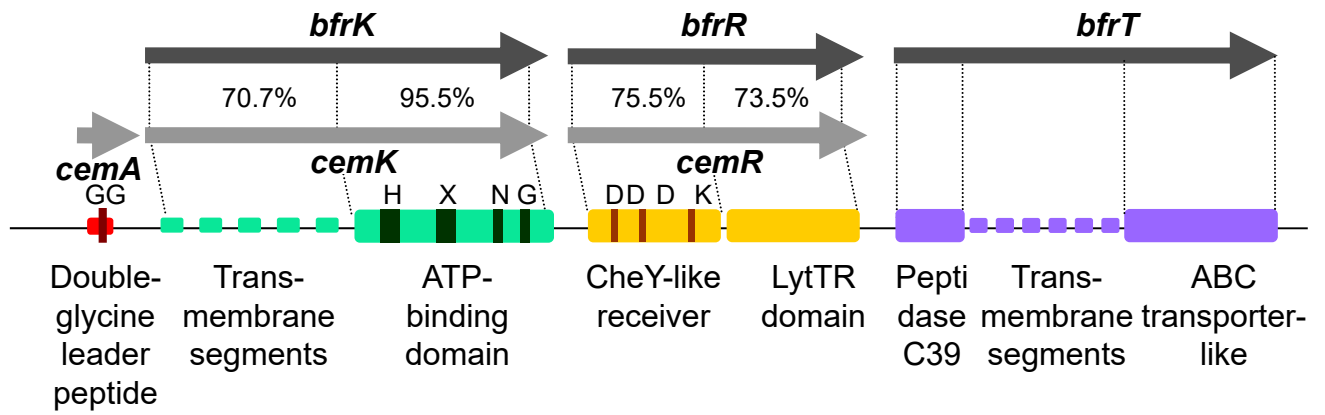


**Figure 1.** Schematic representation of the two-component regulatory systems *bfrKRT* and *cemAKR* operons and their protein and nucleotide sequence analysis. Bioinformatic analysis of histidine kinases BfrK and CemK reveals an amino-terminal transmembrane domain and a carboxyl terminal ATPase-like ATP-binding domain, where the specific homology boxes H, X, N, and G assign features to the HPK<sub>10</sub> subfamily. The functional domains of response regulators BfrR and CemR are predicted as CheY-like superfamily receiver with conserved aspartate (D) and lysine (K) residues at the amino-terminus, along with LytTR DNA-binding domain of the LytR/AlgR family at the carboxyl-terminus. The functional prediction of BfrT shows a bacteriocin processing peptidase C39 domain, transmembrane segments, and ABC transporter-like domain. CemA was identified using the BAGEL program, which also revealed it was a bacteriocin-like autoinducing peptide, which contains a conserved double-glycine (GG) motif in the leader peptide region. Numbers indicate the protein identity of the histidine kinases and response regulators.

**Figure 2.** Su and Gänzle

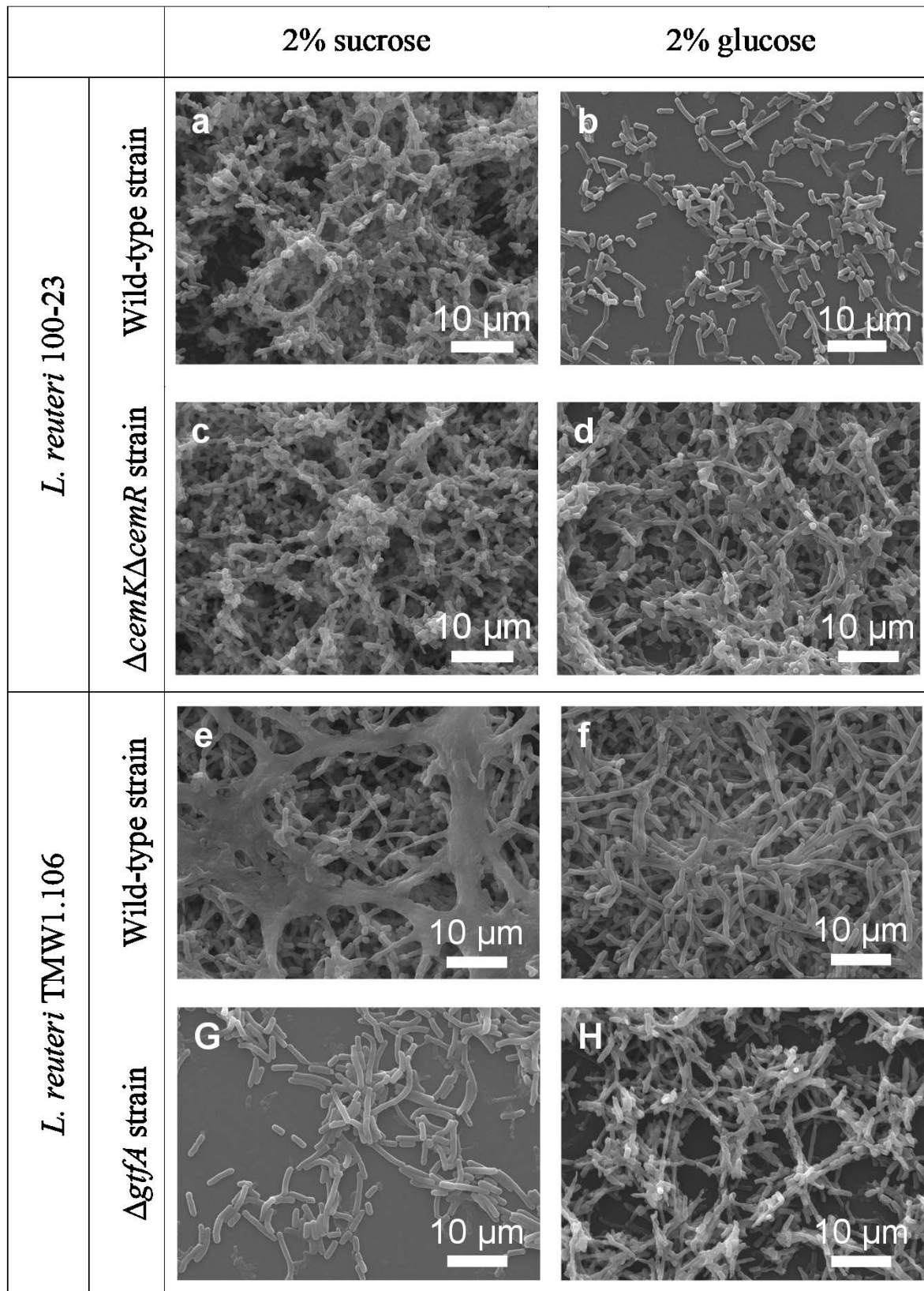




**Figure 2.** SEM micrographs of *L. reuteri* cells on polystyrene surfaces. *L. reuteri* 100-23 (a, b),  $\Delta cemK\Delta cemR$  (c, d), TMW1.106 (e, f), and  $\Delta gtfA$  (g, h) were grown in MRS media containing either 2% sucrose (a, c, e, and g) or 2% glucose (b, d, f, and h). Micrographs were taken from six different fields of two independent experiments. Magnification is  $\times 5000$ .

1

2 **Figure 3.** Su and Gänzle

3

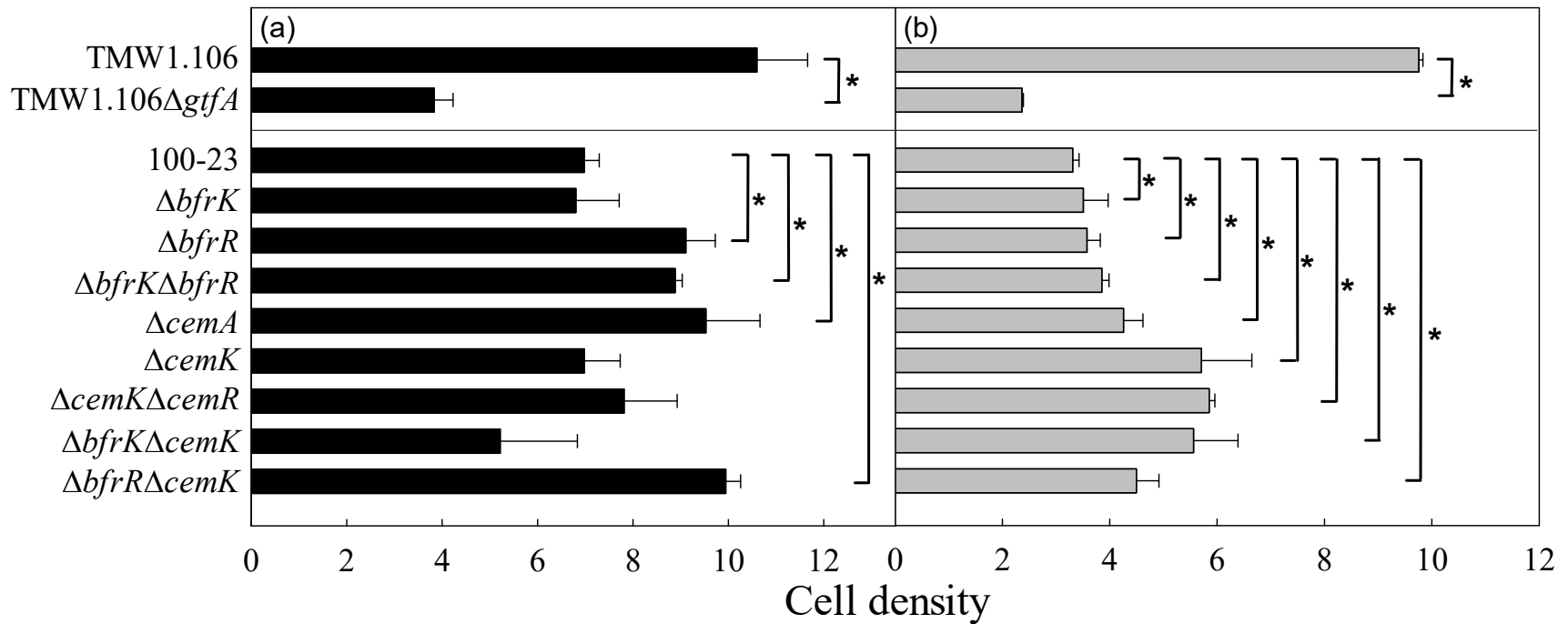
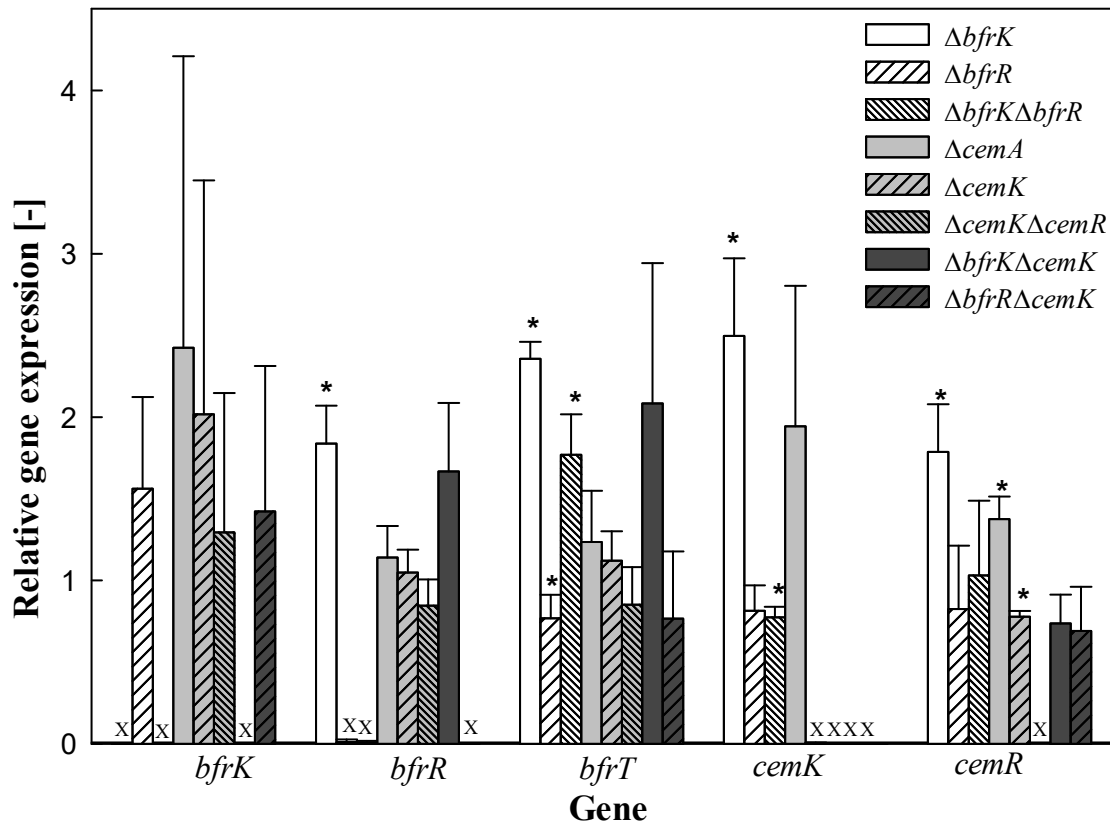


**Figure 3.** Adherence ability of *L. reuteri* on polystyrene plates. Quantitative analysis of cells adhered to polystyrene plates was carried out using cells that were grown over 24 h, which were inoculated in MRS broth containing 2% sucrose (black bar, a) or 2% glucose (grey bar, b). Adherence ability was measured by an optical density of 600 nm. A significant difference between the adherence ability of the mutant strains and the wild-type strains is indicated by asterisk (\*) ( $p < 0.05$ ). Data shown are the means of three independent experiments with standard deviations.



5  
6 **Figure 4.** Relative quantification of gene expression in *L. reuteri* 100-23 and its derived mutant  
7 strains grown in gluMRS. The expressions of the *bfrKRT* and *cemAKR* operons were determined  
8 by qPCR (the y-axis; linear scale) with primers specific to genes *bfrK*, *bfrR*, *bfrT*, *cemK* and  
9 *cemR* (the x-axis). The *L. reuteri* isogenic strains used in this study are  $\Delta bfrK$ ,  $\Delta bfrR$ ,  
10  $\Delta bfrK\Delta bfrR$ ,  $\Delta cemA$ ,  $\Delta cemK$ ,  $\Delta cemK\Delta cemR$ ,  $\Delta bfrK\Delta cemK$ , and  $\Delta bfrR\Delta cemK$ . A significant  
11 difference from the wild-type strain (relative gene expression = 1) is indicated by asterisk (\*) ( $p$   
12 < 0.05). The results are shown as means  $\pm$  the standard deviations of three independent  
13 experiments performed in triplicate. . Primers targeting deleted genes in mutant strains yielded  
14 no amplicons in RT-qPCR reactions; these controls are indicated by the letter “X”.

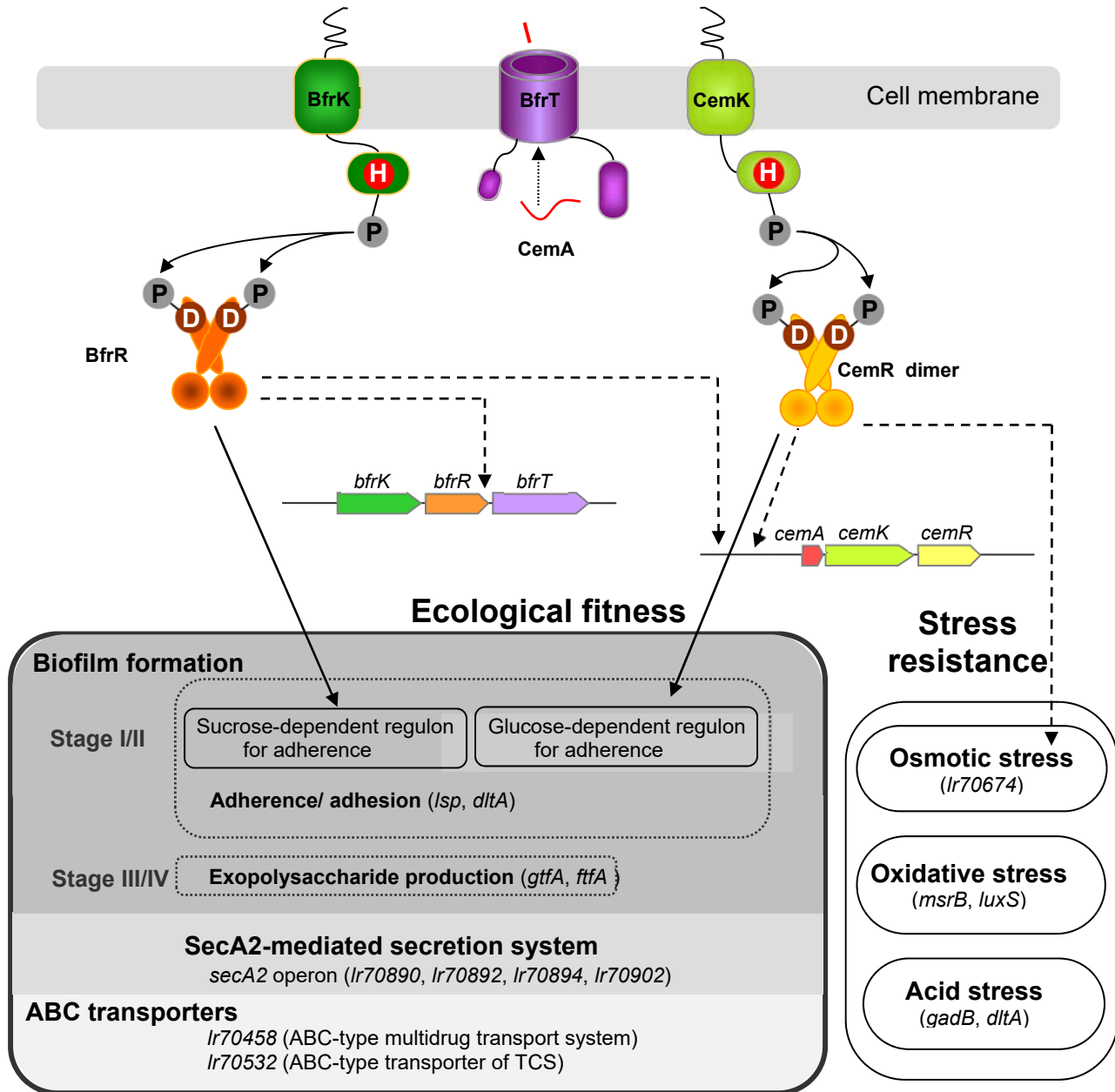


**Figure 5.** Schematic overview of the TCS regulatory signaling cascade of the *bfrKRT* and *cemAKR* operons, and its relationship to the genes related to ecological performance of *L. reuteri* in the intestinal tract of mice. Dashed lines indicate relationships that were established on the basis of quantification of gene expression. The TCS involves signal sensing by a histidine kinase (BfrK, CemK), followed by histidine (H) phosphorylation and phosphotransfer to an aspartate (D) of a response regulator (BfrR, CemR). Disruptions in *bfrKRT* affect expression of *bfrT* as well as genes in the *cemAKR* operon when glucose is the sole carbohydrate source in the growth media; disruption of *cemRK* does not affect expression of *bfrKRT* but alters expression of *cemA* and *lr70674* (osmoprotectant binding protein). Because a transport enzyme is not part of the *cemAKR* system, the maturation of the autoinducing peptide CemA may be processed and transported by the ABC transporter BfrT. Mutations in the *bfrKRT* system as well as *cemA* affected predominantly biofilm formation with sucrose as carbon source while disruption of genes in the *cemAKR* system has a stronger effect on glucose-dependent regulons of biofilm formation.

Adherence of *L. reuteri* to mouse epithelial cells or mediated by *lsp* (Walter *et al.*, 2005). The membrane protein D-alanine-D-ananyl carrier protein ligase (DltA) affects *L. reuteri*'s ability to adhere and to resist acid stress (Walter *et al.*, 2007). Extracellular glucansucrases and levansucrase contribute to biofilm formation *in vitro* and ecological fitness *in vivo* (Walter *et al.*, 2008). Disruption of the *secA2* operon and ABC transporters (*lr70458*, *lr70532*) also impaired colonization of mice by *L. reuteri* (Frese *et al.*, 2011).

Methionine-R-sulfoxide reductase, coded by *msrB* in *L. reuteri* 100-23, is an antioxidant repair enzyme reducing methionine sulfoxide to methionine. Disruption of *msrB* has impairs colonisation of mice by *L. reuteri* (Walter *et al.*, 2005). Disruption of *luxS* in *L. reuteri* 100-23 is associated with the metabolic conversion of S-ribosyl homocysteine to homocysteine but not AI-2 quorum-sensing regulation (Wilson *et al.*, 2012). Genes *gadB* (Su *et al.*, 2011) and *dltA* (Walter *et al.*, 2007) increase acid resistance of *L. reuteri*.